

# 1 Dynamical Mean-Field Approach for Strongly Correlated Materials

Dieter Vollhardt

Center for Electronic Correlations and Magnetism

University of Augsburg

## Contents

<b>1</b>	<b>Introduction</b>	<b>2</b>
1.1	Electronic correlations . . . . .	2
1.2	Hubbard model . . . . .	4
<b>2</b>	<b>Mean-field approaches for many-body systems</b>	<b>5</b>
2.1	Construction of mean-field theories . . . . .	5
2.2	Weiss mean-field theory for the Ising model . . . . .	6
<b>3</b>	<b>Lattice fermions in high dimensions</b>	<b>7</b>
3.1	Simplifications of perturbation theory . . . . .	8
<b>4</b>	<b>Dynamical mean-field theory for correlated lattice fermions</b>	<b>10</b>
4.1	Solving the DMFT self-consistency equations . . . . .	12
<b>5</b>	<b>Mott-Hubbard metal-insulator transition</b>	<b>13</b>
5.1	The characteristic structure of the spectral function . . . . .	14
<b>6</b>	<b>Electronic correlations in materials</b>	<b>17</b>
6.1	LDA+DMFT . . . . .	17
6.2	Single-particle spectrum of correlated electron materials . . . . .	20
<b>7</b>	<b>Summary and outlook</b>	<b>22</b>

# 1 Introduction

## 1.1 Electronic correlations

In physics the average or expectation value of a product of quantities usually differs from the product of the averages of the individual quantities:

$$\langle AB \rangle \neq \langle A \rangle \langle B \rangle. \quad (1)$$

This is attributed to *correlations*. For example, in an interacting system a particle at position  $\mathbf{r}$  will, in general, influence other particles at positions  $\mathbf{r}'$ . Therefore the density-density correlation function of this system does not factorize

$$\langle n(\mathbf{r})n(\mathbf{r}') \rangle \neq \langle n(\mathbf{r}) \rangle \langle n(\mathbf{r}') \rangle = n^2, \quad (2)$$

i.e., is not given by the square of the average density  $n$ . (For quantum particles the unequal sign holds even in the non-interacting case, since the quantum statistics by itself already leads to a spatial dependence). Correlations are thus defined as effects which go beyond factorization approximations such as Hartree or Hartree-Fock theory.

Correlations in space and time are by no means abstract notions, but occur frequently in everyday life. Persons in an elevator or in a car are strongly correlated both in space and time, and it would be quite inadequate to describe the situation of a person in such a case within a factorization approximation where the influence of the other person(s) is described only by a static mean-field, i.e., a structureless cloud.

As in the case of two persons riding together on an elevator, two electrons with different spin direction occupying the same narrow  $d$  or  $f$  orbital in a real material are also correlated. Here the degree of correlation can be estimated in a very simplified picture as follows. Assuming the correlated electrons (or rather the quasiparticles, i.e., excitations) to have a well-defined dispersion  $\epsilon_{\mathbf{k}}$ , their velocity is given by  $v_{\mathbf{k}} = \frac{1}{\hbar} |\nabla_{\mathbf{k}} \epsilon_{\mathbf{k}}|$ . The typical velocity is given by  $v_{\mathbf{k}} \sim \frac{a}{\tau}$ , where  $a$  is the lattice spacing and  $\tau$  is the average time spent on an atom. The derivative can be estimated as  $\frac{1}{\hbar} |\nabla_{\mathbf{k}} \epsilon_{\mathbf{k}}| \sim \frac{1}{\hbar} aW$  since  $|\nabla_{\mathbf{k}}| \sim 1/k \sim a$  and  $|\epsilon_{\mathbf{k}}|$  corresponds to the band overlap  $t$  and hence to the band width  $W$ . Altogether this means that

$$\tau \sim \frac{\hbar}{W}. \quad (3)$$

The narrower a band, the longer an electron therefore resides on an atom and thereby feels the presence of other electrons. Hence a narrow band width implies strong electronic correlations. This is the case for many elements in the periodic table. Namely, in many materials with partially filled  $d$  and  $f$  electron shells, such as the transition metals V, Fe, and Ni and their oxides, or rare-earth metals such as Ce, electrons occupy narrow orbitals. This spatial confinement enhances the effect of the Coulomb interaction between the electrons, making them “strongly correlated”. Correlations give rise to profound quantitative and qualitative changes of the physical properties of electronic systems as compared to non-interacting particles. Indeed, already in 1937, at the outset of modern solid state physics, de Boer and Verwey [1] drew attention

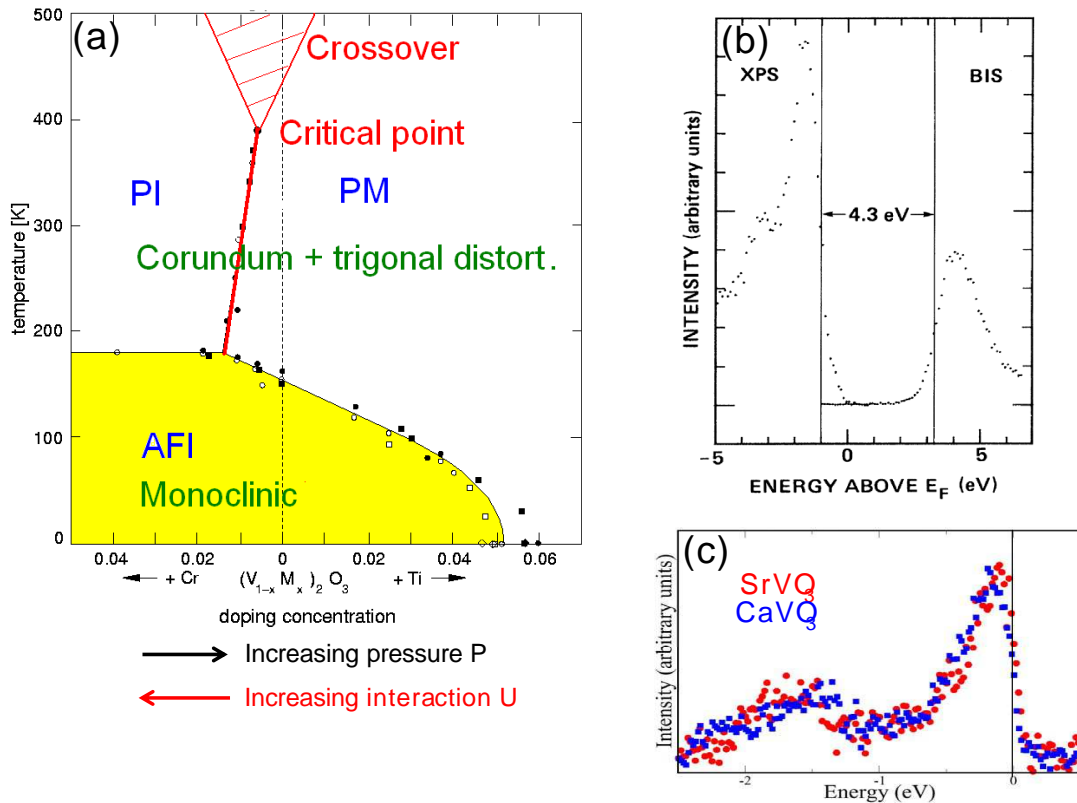


**Fig. 1:** Typical correlation effects in solids: (a) Mott- Hubbard metal-insulator transition in the paramagnetic phase of  $V_2O_3$  doped with Cr (after [3]); (b) insulating energy gap at the Fermi surface of NiO (after [4]); (c) lower Hubbard band in  $SrVO_3$  and  $CaVO_3$  due to transfer of spectral weight from the Fermi energy to energies around  $-1.7$  eV (after [5])

to the surprising properties of materials with incompletely filled  $3d$ -bands, such as NiO. This observation prompted Mott and Peierls [2] to consider the interaction between the electrons.

Correlations may, for example, lead to a transition from metallic to insulating behavior as in  $V_2O_3$  or NiO (see Fig. 1 (a),(b)). In particular, correlated materials often respond very strongly to changes in external parameters. This is expressed by large renormalizations of the response functions of the system, e.g., of the spin susceptibility and the charge compressibility, and by a strong transfer of spectral weight (see Fig. 1 (c)). Electronic correlations also play an essential role in high temperature superconductivity. In particular, the interplay between the spin, charge and orbital degrees of freedom of the correlated  $d$  and  $f$  electrons and with the lattice degrees of freedom leads to a wealth of unusual phenomena at low temperatures [6]. These properties cannot be explained within conventional mean-field theories, e.g., Hartree-Fock theory, since they describe the interaction only in an average way.

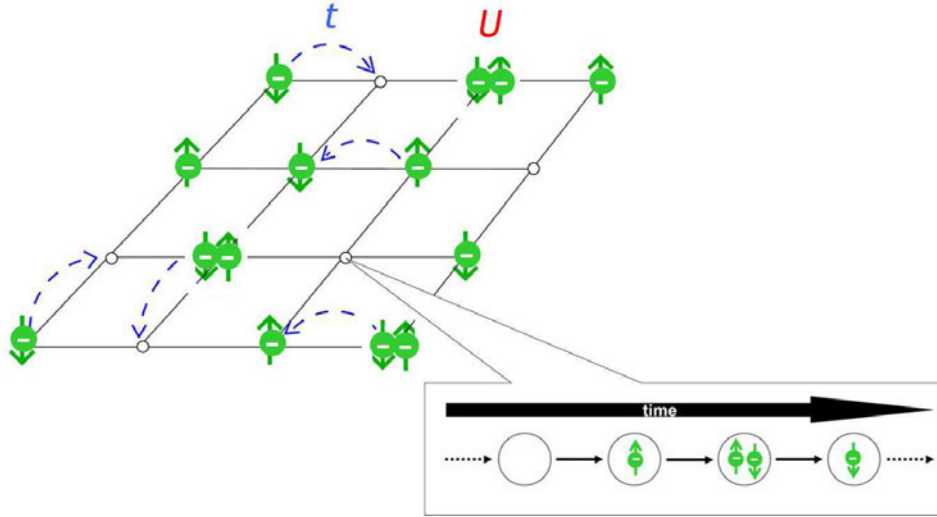


**Fig. 2:** Schematic illustration of interacting electrons in a solid in terms of the Hubbard model. The ions appear only as a rigid lattice (here represented as a square lattice). The electrons, which have a mass, a negative charge, and a spin ( $\uparrow$  or  $\downarrow$ ), move from one lattice site to the next with a hopping amplitude  $t$ . The quantum dynamics thus leads to fluctuations in the occupation of the lattice sites as indicated by the time sequence. When two electrons meet on a lattice site (which is only possible if they have opposite spin because of the Pauli exclusion principle) they encounter an interaction  $U$ . A lattice site can either be unoccupied, singly occupied ( $\uparrow$  or  $\downarrow$ ), or doubly occupied.

## 1.2 Hubbard model

The simplest model describing interacting electrons in a solid is the one-band, spin-1/2 Hubbard model [7–9] where the interaction between the electrons is assumed to be so strongly screened that it is taken as purely local. The Hamiltonian consists of two terms, the kinetic energy  $\hat{H}_0$  and the interaction energy  $\hat{H}_I$  (here and in the following operators are denoted by a hat):

$$\hat{H} = \hat{H}_0 + \hat{H}_I \quad (4a)$$

$$\hat{H}_0 = \sum_{\mathbf{R}_i, \mathbf{R}_j} \sum_{\sigma} t_{ij} \hat{c}_{i\sigma}^{\dagger} \hat{c}_{j\sigma} = \sum_{\mathbf{k}, \sigma} \epsilon_{\mathbf{k}} \hat{n}_{\mathbf{k}\sigma} \quad (4b)$$

$$\hat{H}_I = U \sum_{\mathbf{R}_i} \hat{n}_{i\uparrow} \hat{n}_{i\downarrow}, \quad (4c)$$

where  $\hat{c}_{i\sigma}^{\dagger}$  ( $\hat{c}_{i\sigma}$ ) are creation (annihilation) operators of electrons with spin  $\sigma$  at site  $\mathbf{R}_i$ , and  $\hat{n}_{i\sigma} = \hat{c}_{i\sigma}^{\dagger} \hat{c}_{i\sigma}$ . The Fourier transform of the kinetic energy in (4b), where  $t_{ij}$  is the hopping amplitude, involves the dispersion  $\epsilon_{\mathbf{k}}$  and the momentum distribution operator  $\hat{n}_{\mathbf{k}\sigma}$ .

A schematic picture of the Hubbard model is shown in Fig. 2. When we look only at a single site of this lattice model, this site will sometimes be empty, singly occupied or doubly occupied. In particular, for strong repulsion  $U$  double occupations are energetically very unfavorable and are therefore strongly suppressed. In this situation  $\langle \hat{n}_{i\uparrow} \hat{n}_{i\downarrow} \rangle$  must not be factorized

since  $\langle \hat{n}_{i\uparrow} \hat{n}_{i\downarrow} \rangle \neq \langle \hat{n}_{i\uparrow} \rangle \langle \hat{n}_{i\downarrow} \rangle$ . Otherwise, correlation phenomena such as the Mott-Hubbard metal-insulator transition are eliminated from the very beginning. This explains why Hartree-Fock-type mean-field theories are generally insufficient to explain the physics of electrons in the paramagnetic phase for strong interactions.

The Hubbard model looks very simple. However, the competition between the kinetic energy and the interaction leads to a complicated many-body problem.

## 2 Mean-field approaches for many-body systems

### 2.1 Construction of mean-field theories

It is well known that theoretical investigations of quantum-mechanical many-body systems are faced with severe technical problems, particularly in those dimensions which are most interesting to us, i. e.,  $d = 2, 3$ . This is due to the complicated dynamics and, in the case of fermions, the non-trivial algebra introduced by the Pauli exclusion principle. In the absence of exact methods there is clearly a great need for reliable, controlled approximation schemes.

In the statistical theory of classical and quantum-mechanical systems a rough, overall description of the properties of a model is often provided by a *mean-field theory*. Although the term is frequently used it is rather vague since there is no unique construction scheme.

There does exist a well-established route to mean-field theories which makes use of the simplifications that occur when some parameter is taken to be large (in fact, infinite), e.g., the length of the spins  $S$ , the spin degeneracy  $N$ , or the coordination number  $Z$  (the number of nearest neighbors of a lattice site<sup>1</sup>). Investigations in this limit, supplemented, if at all possible, by an expansion in the inverse of the large parameter, often provide valuable insight into the fundamental properties of a system even when this parameter is not large.

One of the best-known theories of this kind is the Weiss molecular-field theory for the Ising model [10]. It is a prototypical *single-site mean-field theory* which becomes exact for infinite-range interaction, as well as in the limit of the coordination number  $Z \rightarrow \infty$  or<sup>2</sup> the spatial dimension  $d \rightarrow \infty$ . In the latter case  $1/Z$  or  $1/d$  is a small parameter which can sometimes be used to improve the mean-field theory systematically. This mean-field theory contains no

---

<sup>1</sup>In three dimensions ( $d = 3$ ) one has  $Z = 6$  for a simple cubic lattice ( $Z = 2d$  for a hypercubic lattice in general dimensions  $d$ ),  $Z = 8$  for a bcc lattice and  $Z = 12$  for an fcc-lattice. Since  $Z \sim \mathcal{O}(10)$  is already quite large in  $d = 3$ , such that  $1/Z$  is rather small, it is only natural and in the general spirit of theoretical physics to consider the extreme limit  $Z \rightarrow \infty$  to simplify the problem. Later, if possible, one can try to improve the result by expanding in the small parameter  $1/Z$ . It turns out that several standard approximation schemes which are commonly used to explain experimental results in dimension  $d = 3$ , are exact only in  $d = \infty$  (for a more detailed discussion see Ref. [11]).

<sup>2</sup>For regular lattices, e.g., Bravais-lattices, both a dimension  $d$  and a coordination number  $Z$  can be defined. In this case either  $d$  or  $Z$  can be used alternatively as an expansion parameter. However, there exist other lattices (or rather graphs) which cannot be associated with a physical dimension  $d$  although a coordination number  $Z$  is well-defined. The best-known example is the Bethe lattice, an infinitely extended Cayley tree [10, 12], which is not a regular lattice because it does not have loops. The coordination number  $Z$  is therefore a very useful parameter for theoretical investigations of lattice models, although the dimension  $d$  is the more general physical parameter. In the following discussion we mostly use both  $d$  and  $Z$  in parallel.

unphysical singularities and is applicable for all values of the input parameters, i.e., coupling parameters, magnetic field, and temperature. It is also diagrammatically controlled [13]. Insofar it is a very respectable approximation which sets very high standards for other mean-field theories.

## 2.2 Weiss mean-field theory for the Ising model

The Ising model with nearest-neighbor (NN) coupling is defined by

$$H = -\frac{1}{2}J \sum_{\langle \mathbf{R}_i, \mathbf{R}_j \rangle} S_i S_j, \quad (5)$$

where we assume ferromagnetic coupling ( $J > 0$ ). Every spin  $S_i$  interacts with a local field  $h_i$ , produced by its nearest neighbors at site  $\mathbf{R}_i$ . In the Weiss mean-field approach the two-spin interaction in (5) is decoupled, i. e.,  $H$  is replaced by a mean-field Hamiltonian

$$H^{\text{MF}} = -h_{\text{MF}} \sum_{\mathbf{R}_i} S_i + E_{\text{shift}}. \quad (6a)$$

Now a spin  $S_i$  interacts only with a global (“molecular”) field

$$h_{\text{MF}} = J \sum_{\mathbf{R}_j}^{(i)} \langle S_j \rangle \quad (6b)$$

$$\equiv J Z \langle S \rangle. \quad (6c)$$

Here  $\langle \rangle$  indicates the thermal average,  $E_{\text{shift}} = \frac{1}{2} L J Z \langle S \rangle^2$  is a constant energy shift with  $L$  as the number of lattice sites, and the superscript  $(i)$  implies summation over NN-sites of  $\mathbf{R}_i$ . This corresponds to the factorization

$$\langle [S_i - \langle S \rangle][S_j - \langle S \rangle] \rangle \equiv 0, \quad (7)$$

whereby correlated fluctuations of spins at sites  $\mathbf{R}_i$  and  $\mathbf{R}_j$  are neglected. In the limit  $Z \rightarrow \infty$  the coupling constant  $J$  has to be rescaled as

$$J \rightarrow \frac{J^*}{Z}, \quad J^* = \text{const} \quad (8)$$

for  $h_{\text{MF}}$  to remain finite. In this limit the factorization procedure (7), and hence the replacement of (5), by the mean-field Hamiltonian (6a), becomes exact [14, 15].

Eq. (6a) implies that in the limit  $Z \rightarrow \infty$  fluctuations in the bath of surrounding neighbors become unimportant, such that the surrounding of any site is completely described by a single mean-field parameter  $h_{\text{MF}}$  (see Fig. 3). Hence the Hamiltonian becomes purely local

$$H^{\text{MF}} = \sum_{\mathbf{R}_i} H_i + E_{\text{shift}} \quad (9)$$

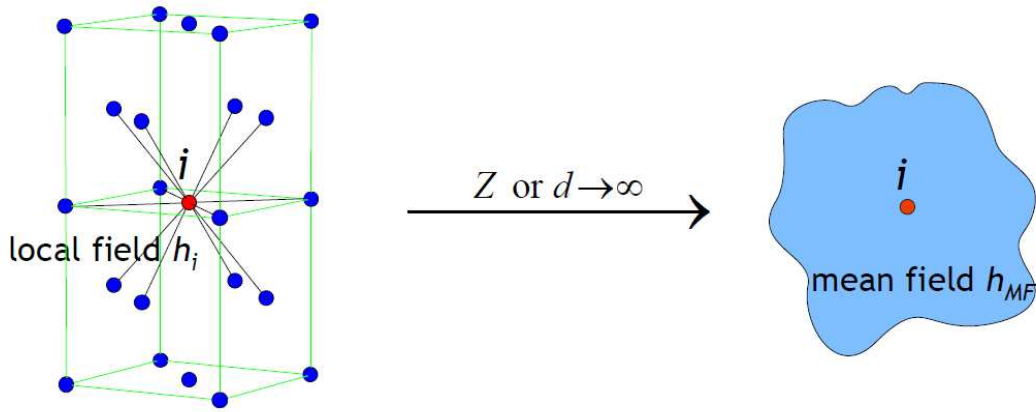


**Fig. 3:** Already in three dimensions ( $d = 3$ ) the coordination number  $Z$  of a lattice can be quite high, as in the face-centered cubic lattice where  $Z = 12$ . In the limit  $Z \rightarrow \infty$ , or equivalently  $d \rightarrow \infty$ , the Ising model effectively reduces to a single-site problem where the local field  $h_i$  is replaced by a global mean (“molecular”) field  $h_{MF}$ .

$$H_i = -h_{MF} S_i. \quad (10)$$

Thereby the problem reduces to an effective *single-site problem*. The value of  $\langle S \rangle$  is determined by the self-consistent equation

$$\langle S \rangle = \tanh(\beta J^* \langle S \rangle), \quad (11)$$

where  $\beta = 1/T$  (here  $k_B = 1$ ).

### 3 Lattice fermions in high dimensions

It is natural to ask whether the limit  $d \rightarrow \infty$  may also be useful in the investigation of lattice models with itinerant quantum-mechanical degrees of freedom and, in particular, in the case of the Hubbard model. Following Ref. [16] we take a look at the kinetic energy term (4b), since the interaction term is purely local and is thereby completely independent of the lattice structure and the dimension. For nearest-neighbor hopping on a  $d$ -dimensional hypercubic lattice (where  $Z = 2d$ )  $\epsilon_{\mathbf{k}}$  is given by<sup>3</sup>

$$\epsilon_{\mathbf{k}} = -2t \sum_{i=1}^d \cos k_i. \quad (12)$$

The density of states (DOS) corresponding to  $\epsilon_{\mathbf{k}}$  is

$$N_d(\omega) = \sum_{\mathbf{k}} \delta(\hbar\omega - \epsilon_{\mathbf{k}}). \quad (13)$$

This is simply the probability density for finding  $\omega = \epsilon_{\mathbf{k}}$  for a random choice of  $\mathbf{k} = (k_1, \dots, k_d)$ . If the  $k_i$  are chosen randomly,  $\epsilon_{\mathbf{k}}$  in (12) is the sum of (independent) random numbers  $-2t \cos k_i$ .

<sup>3</sup>In the following we set Planck’s constant  $\hbar$ , Boltzmann’s constant  $k_B$ , and the lattice spacing equal to unity.

The central limit theorem then implies that in the limit  $d \rightarrow \infty$  the DOS is given by a Gaussian

$$N_d(\omega) \xrightarrow{d \rightarrow \infty} \frac{1}{2t\sqrt{\pi d}} \exp \left[ - \left( \frac{\omega}{2t\sqrt{d}} \right)^2 \right]. \quad (14)$$

Unless  $t$  is scaled properly with  $d$  this DOS will become arbitrarily broad and featureless for  $d \rightarrow \infty$ . Clearly only the scaling of the hopping amplitude

$$t \rightarrow \frac{t^*}{\sqrt{d}}, \quad t^* = \text{const.}, \quad (15)$$

yields a non-trivial DOS [17, 16]:

$$N_\infty(\omega) = \frac{1}{\sqrt{2\pi t^*}} \exp \left[ - \frac{1}{2} \left( \frac{\omega}{t^*} \right)^2 \right]. \quad (16)$$

By contrast, the interaction term in (4) is purely local and independent of the surrounding. Hence it is independent of the spatial dimension of the system. Consequently, the on-site interaction  $U$  need not be scaled. So we see that the scaled Hubbard Hamiltonian

$$\hat{H} = - \frac{t^*}{\sqrt{Z}} \sum_{\langle \mathbf{R}_i, \mathbf{R}_j \rangle} \sum_{\sigma} \hat{c}_{i\sigma}^\dagger \hat{c}_{j\sigma} + U \sum_{\mathbf{R}_i} \hat{n}_{i\uparrow} \hat{n}_{i\downarrow} \quad (17)$$

has a nontrivial  $Z \rightarrow \infty$  limit, where both terms, the kinetic energy and the interaction, are of the same order of magnitude and are thereby able to compete. It is this competition between the two terms which leads to interesting many-body physics.<sup>4</sup>

The scaling (15) was determined within a  $\mathbf{k}$ -space formulation. We will now derive the same result within a position-space formulation.

### 3.1 Simplifications of perturbation theory

The most important consequence of the scaling (15) is the fact that it leads to significant simplifications in the investigation of Hubbard-type lattice models [16, 18–22]; for details see Ref. [11]. To understand this point better we take a look at the perturbation theory in terms of  $U$ . At  $T = 0$  and  $U = 0$  the kinetic energy of the Hubbard model may be written as

$$E_{\text{kin}}^0 = -t \sum_{\langle \mathbf{R}_i, \mathbf{R}_j \rangle} \sum_{\sigma} g_{ij,\sigma}^0 \quad (18)$$

---

<sup>4</sup>To obtain a physically meaningful mean-field theory for a model its internal or free energy has to remain finite in the limit  $d$  or  $Z \rightarrow \infty$ . While in the case of the Ising model the scaling  $J \rightarrow \tilde{J}/Z$ ,  $\tilde{J} = \text{const.}$ , was rather obvious this is not so for more complicated models. Namely, quantum many-particle systems are usually described by a Hamiltonian consisting of several non-commuting terms, e.g., a kinetic energy and an interaction, each of which is associated with a coupling parameter, usually a hopping amplitude and an interaction, respectively. In such a case the question of how to scale these parameters has no unique answer since this depends on the physical effects one wishes to explore. In any case, the scaling should be performed such that the model remains non-trivial and that its internal or free energy stays finite in the  $Z \rightarrow \infty$  limit. By “non-trivial” we mean that not only  $\langle \hat{H}_0 \rangle$  and  $\langle \hat{H}_{\text{int}} \rangle$ , but also the *competition* between these terms, expressed by  $\langle [\hat{H}_0, \hat{H}_{\text{int}}] \rangle$ , should remain finite. In the case of the Hubbard model it would be possible to employ the scaling  $t \rightarrow t^*/Z$ ,  $t^* = \text{const.}$ , but then the kinetic energy would be reduced to zero in the limit  $d \rightarrow \infty$ , making the resulting model uninteresting (but not unphysical) for most purposes.

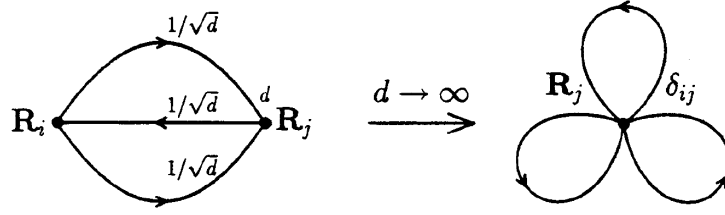


**Fig. 4:** Contribution to the irreducible self-energy for the Hubbard model in second-order perturbation theory in  $U$ , and its collapse in the limit  $d \rightarrow \infty$ .

where  $g_{ij,\sigma}^0 = \langle \hat{c}_{i\sigma}^\dagger \hat{c}_{j\sigma} \rangle_0$  is the one-particle density matrix. This quantity can also be interpreted as the amplitude for transitions between site  $\mathbf{R}_i$  and  $\mathbf{R}_j$ , whose square is proportional to the probability for a particle to hop from  $\mathbf{R}_j$  to  $\mathbf{R}_i$ , i.e.,  $|g_{ij,\sigma}^0|^2 \sim 1/Z \sim 1/d$  since  $\mathbf{R}_j$  has  $\mathcal{O}(d)$  nearest neighbors  $\mathbf{R}_i$ . Thus the sum of  $|g_{ij,\sigma}^0|^2$  over all nearest neighbors must yield a constant. In the limit  $d \rightarrow \infty$  we then have

$$g_{ij,\sigma}^0 \sim \mathcal{O}\left(\frac{1}{\sqrt{d}}\right), \quad \mathbf{R}_i \text{ NN of } \mathbf{R}_j. \quad (19)$$

Since the sum over the NN-sites  $\mathbf{R}_i$  in (18) is of  $\mathcal{O}(d)$  the NN-hopping amplitude  $t$  must obviously be scaled according to (15) for  $E_{\text{kin}}^0$  to remain finite in the limit  $d, Z \rightarrow \infty$ . Hence, as expected, a real-space formulation yields the same results for the required scaling of the hopping amplitude.

The one-particle Green function (“propagator”)  $G_{ij,\sigma}^0(\omega)$  of the non-interacting system obeys the same scaling as  $g_{ij,\sigma}^0$ . This follows directly from its definition

$$G_{ij,\sigma}^0(t) \equiv - \left\langle T \hat{c}_{i\sigma}(t) \hat{c}_{j\sigma}^\dagger(0) \right\rangle_0, \quad (20)$$

where  $T$  is the time ordering operator, and the time evolution of the operators is provided by the Heisenberg representation. The one-particle density matrix is obtained as  $g_{ij,\sigma}^0 = \lim_{t \rightarrow 0^-} G_{ij,\sigma}^0(t)$ . If  $g_{ij,\sigma}^0$  obeys (19) the one-particle Green function  $G_{ij,\sigma}^0(t)$  must follow the same scaling at all times since this property does not depend on the time evolution and the quantum mechanical representation. The Fourier transform  $G_{ij,\sigma}^0(\omega)$  also preserves this property.

Although the propagator  $G_{ij,\sigma}^0 \sim 1/\sqrt{d}$  vanishes for  $d \rightarrow \infty$ , the particles are not localized in this limit. Namely, even in the limit  $d \rightarrow \infty$  the off-diagonal elements of  $G_{ij,\sigma}^0$  contribute, since a particle may hop to  $d$  nearest neighbors with amplitude  $t^*/\sqrt{2d}$ . For general  $i, j$  one finds [23, 19]

$$G_{ij,\sigma}^0 \sim \mathcal{O}\left(1/d^{\|\mathbf{R}_i - \mathbf{R}_j\|/2}\right), \quad (21)$$

where  $\|\mathbf{R}\| = \sum_{n=1}^d |R_n|$  is the length of  $\mathbf{R}$  in the so-called “Manhattan metric”.

It is the property (21) which is the origin of all simplifications arising in the limit  $d \rightarrow \infty$ . In particular, it implies the collapse of all connected, irreducible perturbation theory diagrams in position space [16, 18, 19]. This is illustrated in Fig. 4, where a contribution in second-order perturbation theory to the irreducible self-energy,  $\Sigma_{ij}^{(2)}$ , is shown. As a consequence the full,

irreducible self-energy becomes a purely local quantity [16, 18]:

$$\Sigma_{ij,\sigma}(\omega) \stackrel{d \rightarrow \infty}{\equiv} \Sigma_{ii,\sigma}(\omega) \delta_{ij}. \quad (22a)$$

In the paramagnetic phase we may write  $\Sigma_{ii,\sigma}(\omega) \equiv \Sigma(\omega)$ . The Fourier transform of  $\Sigma_{ij,\sigma}$  is seen to become momentum-independent

$$\Sigma_{\sigma}(\mathbf{k}, \omega) \stackrel{d \rightarrow \infty}{\equiv} \Sigma_{\sigma}(\omega). \quad (22b)$$

This leads to tremendous simplifications in all many-body calculations for the Hubbard model and related models.

Due to the simplifications caused by (22), the most important obstacle for actual diagrammatic calculations in finite dimensions  $d \geq 1$ , namely the integration over intermediate momenta, is removed in  $d = \infty$ . While in finite dimensions these integrations lead to untractable technical problems, they become simple in  $d = \infty$ . In spite of the simplifications in position (or momentum) space the problem retains its full dynamics in  $d = \infty$ .

## 4 Dynamical mean-field theory for correlated lattice fermions

Itinerant quantum mechanical models such as the Hubbard model and its generalizations are much more complicated than classical, Ising-type models. Generally there do not even exist semiclassical approximations for such models that might serve as a starting point for further investigations. Under such circumstances the construction of a mean-field theory with the comprehensive properties of the Weiss molecular field theory for the Ising model will necessarily be much more complicated, too. As discussed above there do exist well-known mean-field approximation schemes, e. g. Hartree-Fock, random-phase approximation, saddle-point evaluations of path integrals, decoupling of operators. However, these approximations do not provide mean-field theories in the spirit of statistical mechanics, since they are not able to give a global description of a given model (e.g., the phase diagram, thermodynamics, etc.) in the entire range of input parameters.

Here the limit of high spatial dimensions  $d$  or coordination number  $Z$  has again been extremely useful [16]. It provides the basis for the construction of a comprehensive mean-field theory for lattice fermions which is diagrammatically controlled and whose free energy has no unphysical singularities. The construction is based on the scaled Hamiltonian (26) and the simplifications in the many-body perturbation theory discussed in Sec. 3.2. There we saw that the local propagator  $G(\omega)$ , i.e., the amplitude for an electron to return to a lattice site, and the local but dynamical self-energy  $\Sigma(\omega)$  are the two central quantities in such a theory. Since the self-energy is a dynamical variable (in contrast to Hartree-Fock theory where it is merely a static potential) the resulting mean-field theory will also be dynamical and can thus describe genuine correlation effects.

The self-consistency equations of this *dynamical mean-field theory* (DMFT) [24–30] for correlated lattice fermions can be derived in different ways; for a discussion see Chapter 4 of

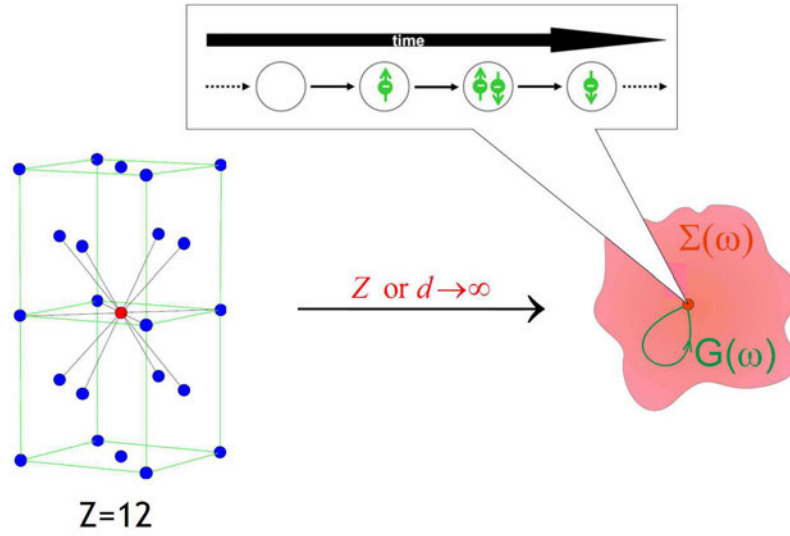


**Fig. 5:** In the limit  $Z \rightarrow \infty$  the Hubbard model effectively reduces to a dynamical single-site problem, which may be viewed as a lattice site embedded in a dynamical mean field. Electrons may hop from the mean field onto this site and back, and interact on the site as in the original Hubbard model (see Fig. 2). The local propagator  $G(\omega)$  (i.e., the return amplitude) and the dynamical self-energy  $\Sigma(\omega)$  of the surrounding mean field play the main role in this limit. The quantum dynamics of the interacting electrons is still described exactly.

Ref. [31]. However, all derivations make use of the fact that in the limit of high spatial dimensions Hubbard-type models reduce to a dynamical single-site problem, where the  $d$ -dimensional lattice model is effectively described by the dynamics of the correlated fermions on a single site which is embedded in a bath provided by the other particles.

Today's standard derivation is based on the mapping of the lattice problem onto a self-consistent single-impurity Anderson model; for details see Ref. [29]. As such it makes contact with the theory of Anderson impurities and the Kondo problem — a well-understood branch of many-body physics, for whose solution efficient numerical codes have been developed already in the 1980's, in particular by making use of the quantum Monte-Carlo (QMC) method [32]. The self-consistent DMFT equations are given by

(i) the equation for the *local propagator*  $G_\sigma(i\omega_n)$  which is expressed by a functional integral as

$$G_\sigma(i\omega_n) = -\frac{1}{Z} \int \prod_\sigma Dc_\sigma^* Dc_\sigma [c_\sigma(i\omega_n) c_\sigma^*(i\omega_n)] \exp[-S_{\text{loc}}] \quad (23)$$

with the partition function

$$Z = \int \prod_\sigma Dc_\sigma^* Dc_\sigma \exp[-S_{\text{loc}}], \quad (24)$$

and the local action

$$S_{\text{loc}} = - \int_0^\beta d\tau_1 \int_0^\beta d\tau_2 \sum_\sigma c_\sigma^*(\tau_1) \mathcal{G}_\sigma^{-1}(\tau_1 - \tau_2) c_\sigma(\tau_2) + U \int_0^\beta d\tau c_\uparrow^*(\tau) c_\uparrow(\tau) c_\downarrow^*(\tau) c_\downarrow(\tau), \quad (25)$$

where  $\mathcal{G}_\sigma$  is the effective local propagator (also called “bath Green function”, or “Weiss mean field”<sup>5</sup>) defined by a Dyson-type equation

$$\mathcal{G}_\sigma(i\omega_n) = [[G_\sigma(i\omega_n)]^{-1} + \Sigma_\sigma(i\omega_n)]^{-1}, \quad (26)$$

(ii) and the expression for the *lattice Green function*  $G_{\mathbf{k}\sigma}(i\omega_n)$  given by

$$G_{\mathbf{k}\sigma}(i\omega_n) = \frac{1}{i\omega_n - \epsilon_{\mathbf{k}} + \mu - \Sigma_\sigma(i\omega_n)}, \quad (27)$$

from which, after performing the lattice Hilbert transform, one obtains the local Green function

$$\begin{aligned} G_\sigma(i\omega_n) &= \sum_{\mathbf{k}} G_{\mathbf{k}\sigma}(i\omega_n) \\ &= \int_{-\infty}^{\infty} d\epsilon \frac{N(\omega)}{i\omega_n - \epsilon + \mu - \Sigma_\sigma(i\omega_n)}, \end{aligned} \quad (28)$$

$$(29)$$

which is equal to the local propagator (23). The ionic lattice on which the electrons move and its structure are seen to enter only through the DOS of the non-interacting electrons.

The self-consistent equations can be solved iteratively: Starting with an initial value for the self-energy  $\Sigma_\sigma(i\omega_n)$  one obtains the local propagator  $G_\sigma(i\omega_n)$  from (29) and thereby the bath Green function  $\mathcal{G}_\sigma(i\omega_n)$  from (26). This determines the local action (25) which is needed to compute a new value for the local propagator  $G_\sigma(i\omega_n)$  and, by employing the old self-energy, a new bath Green function, and so on.

## 4.1 Solving the DMFT self-consistency equations

The dynamics of the full Hubbard model (4) remains complicated even in the limit  $d \rightarrow \infty$  because of the purely local nature of the interaction. Hence an exact, analytic evaluation of the self-consistent set of equations for the local propagator  $G_\sigma$  or the effective propagator  $\mathcal{G}_\sigma$  is not possible. A valuable semi-analytic approximation is provided by the “iterated perturbation theory” (IPT) [26,33,29]. Exact evaluations are only feasible when there is no coupling between the frequencies. This is the case, for example, in the Falicov-Kimball model [22, 34].

Solutions of the general DMFT self-consistency equations require extensive numerical methods, in particular quantum Monte Carlo techniques [27,35,36] (for reviews see Refs. [29,37,38], the numerical renormalization group [39,40], exact diagonalization [41–43] and other techniques, which will be discussed later in this school.

---

<sup>5</sup>In principle, the local functions  $\mathcal{G}_\sigma(i\omega_n)$  and  $\Sigma_\sigma(i\omega_n)$  can both be viewed as a “dynamical mean field” acting on particles on a site, since they all appear in the bilinear term of the local action (25).

It quickly turned out that the DMFT is a powerful tool for the investigation of electronic systems with strong correlations. It provides a non-perturbative and thermodynamically consistent approximation scheme for finite-dimensional systems which is particularly valuable for the study of intermediate-coupling problems where perturbative techniques fail [29, 30].

In the remaining part of these lecture notes I shall discuss several applications of the DMFT to problems involving electronic correlations. In particular, I will address the Mott-Hubbard metal-insulator transition, and explain the connection of the DMFT with band-structure methods — the LDA+DMFT scheme — which is the first comprehensive framework for the *ab initio* investigation of correlated electron materials.

## 5 Mott-Hubbard metal-insulator transition

The correlation induced transition between a paramagnetic metal and a paramagnetic insulator, referred to as “Mott-Hubbard metal-insulator transition” (MIT), is one of the most intriguing phenomena in condensed matter physics [44–46]. This transition is a consequence of the competition between the kinetic energy of the electrons and their local interaction  $U$ . Namely, the kinetic energy prefers the electrons to move (a wave effect) which leads to doubly occupied sites and thereby to interactions between the electrons (a particle effect). For large values of  $U$  the doubly occupied sites become energetically very costly. The system may reduce its total energy by localizing the electrons. Hence the Mott transition is a localization-delocalization transition, demonstrating the particle-wave duality of electrons.

Mott-Hubbard MITs are, for example, found in transition metal oxides with partially filled bands near the Fermi level [6]. For such systems band theory typically predicts metallic behavior. The most famous example is  $V_2O_3$  doped with Cr [3,47,48]. In particular, in  $(V_{0.96}Cr_{0.04})_2O_3$  the metal-insulator transition is of first order below  $T = 380$  K [3], with discontinuities in the lattice parameters and in the conductivity. However, the two phases remain isostructural.

Making use of the half-filled, single-band Hubbard model (4) the Mott-Hubbard MIT was studied intensively in the past [44–46]. Important early results were obtained by Hubbard [8, 49] within a Green function decoupling scheme, and by Brinkman and Rice [50] using the Gutzwiller variational method [7, 51], both at zero temperature.<sup>6</sup> Hubbard’s approach yields a continuous splitting of the band into a lower and upper Hubbard band, but cannot describe quasiparticle features. By contrast, the Gutzwiller-Brinkman-Rice approach (for a review see Ref. [53]) gives a good description of the low-energy, quasiparticle behavior, but cannot reproduce the upper and lower Hubbard bands. In the latter approach the MIT is signalled by the disappearance of the quasiparticle peak.

To solve this problem the DMFT has been extremely valuable since it provided detailed insights into the nature of the Mott-Hubbard MIT for all values of the interaction  $U$  and temperature  $T$  [29, 54, 30].

---

<sup>6</sup>The Gutzwiller variational method [7,51] consists of the choice of a simple projected variational wave function (“Gutzwiller wave function”) and a semi-classical evaluation of expectation values in terms of this wave function (“Gutzwiller approximation”). The Gutzwiller approximation becomes exact in the limit  $d \rightarrow \infty$  [52].

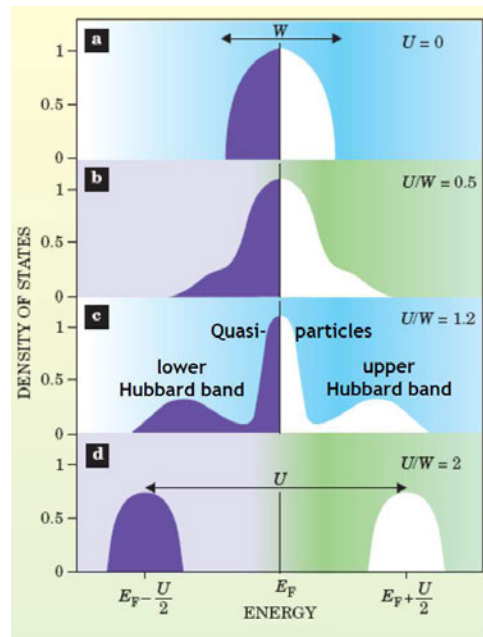


**Fig. 6:** Evolution of the spectral function (“density of states”) of the Hubbard model in the paramagnetic phase at half-filling. a) non-interacting case, b) for weak interactions there is only little transfer of spectral weight away from the Fermi energy, c) for strong interactions a typical three-peak structure consisting of coherent quasiparticle excitations close to the Fermi energy and incoherent lower and upper Hubbard bands is clearly seen, d) above a critical interaction the quasiparticle peak vanishes and the system is insulating, with two well-separated Hubbard bands remaining; after Ref. [30].

## 5.1 The characteristic structure of the spectral function

The Mott-Hubbard MIT is monitored by the spectral function  $A(\omega) = -\frac{1}{\pi}\text{Im}G(\omega + i0^+)$  of the correlated electrons;<sup>7</sup> here we follow the discussion of Refs. [55, 30]. The change of  $A(\omega)$  obtained within the DMFT for the one-band Hubbard model (4) at  $T = 0$  and half filling ( $n = 1$ ) as a function of the Coulomb repulsion  $U$  (measured in units of the bandwidth  $W$  of non-interacting electrons) is shown in Figs. 6 and 7. While Fig. 6 is a schematic picture of the evolution of the spectrum when the interaction is increased, Fig. 7 shows actual numerical results obtained by the NRG [39, 56]. Here magnetic order is assumed to be suppressed (“frustrated”).

While at small  $U$  the system can be described by coherent quasiparticles whose DOS still resembles that of the free electrons, the spectrum in the Mott insulator state consists of two separate incoherent “Hubbard bands” whose centers are separated approximately by the energy  $U$ . The latter originate from atomic-like excitations at the energies  $\pm U/2$  broadened by the hopping of electrons away from the atom. At intermediate values of  $U$  the spectrum then has a characteristic three-peak structure as in the single-impurity Anderson model, which includes both the atomic features (i.e., Hubbard bands) and the narrow quasiparticle peak at low excitation energies, near  $\omega = 0$ . This corresponds to a strongly correlated metal. The structure of the

<sup>7</sup>In the following we only consider the paramagnetic phase.

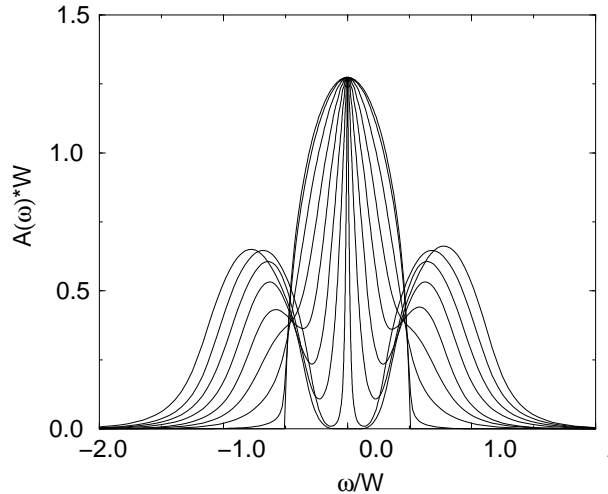


**Fig. 7:** Evolution of the  $T = 0$  spectral function of the one-band Hubbard model with a semi-elliptic (“Bethe”) DOS for interaction values  $U/W = 0, 0.2, 0.4, \dots, 1.6$  ( $W$ : band width) calculated with the numerical renormalization group. At the critical interaction  $U_{c2}/W \simeq 1.47$  the metallic solution disappears and the Mott gap opens; from Ref. [56].

spectrum (lower Hubbard band, quasiparticle peak, upper Hubbard band) is quite insensitive to the specific form of the DOS of the non-interacting electrons.

The width of the quasiparticle peak vanishes for  $U \rightarrow U_{c2}(T)$ . The “Luttinger pinning” at  $\omega = 0$  [20] is clearly observed. On decreasing  $U$ , the transition from the insulator to the metal occurs at a lower critical value  $U_{c1}$ , where the gap vanishes.

It is important to note that the three-peak spectrum originates from a lattice model with only *one* type of electrons. This is in contrast to the single-impurity Anderson model whose spectrum shows very similar features, but is due to *two* types of electrons, namely the localized orbital at the impurity site and the free conduction band. Therefore the screening of the magnetic moment which gives rise to the Kondo effect in impurity systems has a different origin in lattice systems. Namely, as explained by the DMFT, the same electrons provide both the local moments and the electrons which screen these moments [29].

The evolution of the spectral function of the half-filled frustrated Hubbard model at finite temperatures,  $T = 0.0276 W$ , is shown in Fig. 8. This temperature is above the temperature of the critical point so that there is no real transition but only a crossover from a metallic-like to an insulating-like solution. The height of the quasiparticle peak at the Fermi energy is no longer fixed at its zero temperature value. This is due to a finite value of the imaginary part of the self-energy. The spectral weight of the quasiparticle peak is seen to be gradually redistributed and shifted to the upper (lower) edge of the lower (upper) Hubbard band. The inset of Fig. 8 shows the  $U$ -dependence of the value of the spectral function at zero frequency  $A(\omega = 0)$ . For higher values of  $U$  the spectral density at the Fermi level is still finite and vanishes only in the limit  $U \rightarrow \infty$  (or for  $T \rightarrow 0$ , provided that  $U > U_{c2}(T = 0)$ ).

For the insulating phase DMFT predicts the filling of the Mott-Hubbard gap with increasing temperature. This is due to the fact that the insulator and the metal are not distinct phases in

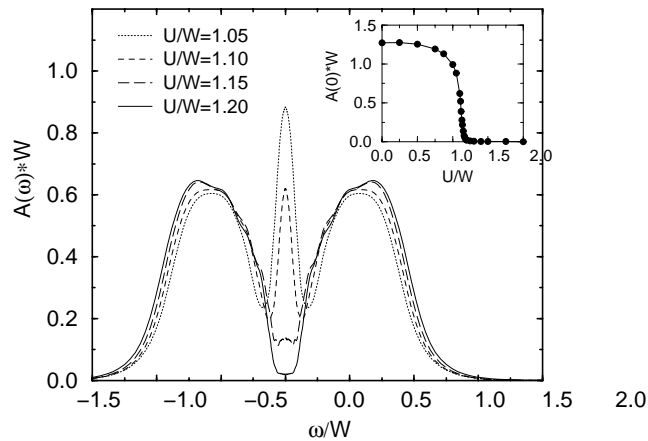


**Fig. 8:** Spectral function for the half-filled Hubbard model for various values of  $U$  at  $T = 0.0276 W$  in the crossover region. The crossover from the metal to the insulator occurs via a gradual suppression of the quasiparticle peak at  $\omega = 0$ . The inset shows the  $U$  dependence of  $A(\omega = 0)$ , in particular the rapid decrease for  $U \approx 1.1 W$ ; from Ref. [55].

the crossover regime, implying that the insulator has a finite spectral weight at the Fermi level. Altogether, the thermodynamic transition line  $U_c(T)$  corresponding to the Mott-Hubbard MIT is found to be of first order at finite temperatures, being associated with a hysteresis region in the interaction range  $U_{c1} < U < U_{c2}$  where  $U_{c1}$  and  $U_{c2}$  are the values at which the insulating and metallic solution, respectively, vanishes [29, 39, 57, 55, 58, 54]. The state-of-the-art MIT phase diagram [54] is shown in Fig. 9. The hysteresis region terminates at a critical point. For higher temperatures the transition changes into a smooth crossover from a bad metal to a bad insulator.

It is interesting to note that the slope of the phase transition line is negative down to  $T = 0$ , which implies that for constant interaction  $U$  the metallic phase can be reached from the insulator by decreasing the temperature  $T$ , i.e., by *cooling*. This anomalous behavior (which corresponds to the Pomeranchuk effect [59] in  $^3\text{He}$ , if we associate solid  $^3\text{He}$  with the insulator and liquid  $^3\text{He}$  with the metal) can be easily understood from the Clausius-Clapeyron equation  $dU/dT = \Delta S/\Delta D$ . Here  $\Delta S$  is the difference between the entropy in the metal and in the insulator, and  $\Delta D$  is the difference between the number of doubly occupied sites in the two phases. Within the single-site DMFT there is no exchange coupling  $J$  between the spins of the electrons in the insulator, since the scaling (15) implies  $J \propto -t^2/U \propto 1/d \rightarrow 0$  for  $d \rightarrow \infty$ . Hence the entropy of the macroscopically degenerate insulating state is  $S_{\text{ins}} = k_B \ln 2$  per electron down to  $T = 0$ . This is larger than the entropy  $S_{\text{met}} \propto T$  per electron in the Landau Fermi-liquid describing the metal, i.e.,  $\Delta S = S_{\text{met}} - S_{\text{ins}} < 0$ . At the same time the number of doubly occupied sites is lower in the insulator than in the metal, i.e.,  $\Delta D = D_{\text{met}} - D_{\text{ins}} > 0$ . The Clausius-Clapeyron equation then implies that the phase-transition line  $T$  vs.  $U$  has a negative slope down to  $T = 0$ . However, this is an artifact of the single-site DMFT. Namely, there will always exist an exchange coupling between the electrons leading to a vanishing entropy of the insulator at  $T = 0$ . Since the entropy of the insulator vanishes faster

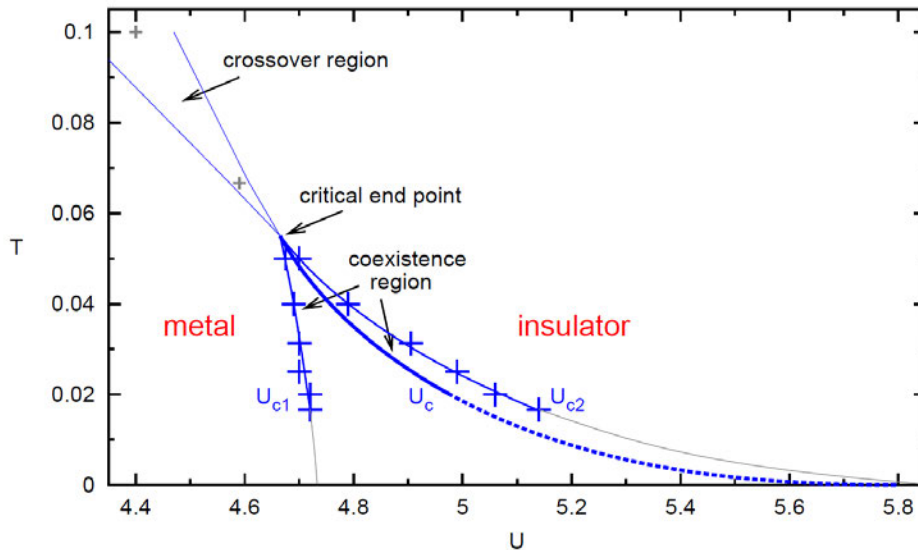


**Fig. 9:** Mott-Hubbard MIT phase diagram showing the metallic phase and the insulating phase, respectively, at temperatures below the critical end point, as well as a coexistence region; from Ref. [54].

than linearly with the temperature, the difference  $\Delta S = S_{\text{met}} - S_{\text{ins}}$  eventually becomes positive, whereby the slope also becomes positive at lower temperatures;<sup>8</sup> this is indeed observed in cluster DMFT calculations [60]. Since  $\Delta S = 0$  at  $T = 0$  the phase boundary must terminate at  $T = 0$  with infinite slope.

At half filling and for bipartite lattices in dimensions  $d > 2$  (in  $d = 2$  only at  $T = 0$ ), the paramagnetic phase is unstable against antiferromagnetic long-range order. The metal-insulator transition is then completely hidden by the antiferromagnetic insulating phase, as shown in Fig. 10.

## 6 Electronic correlations in materials

### 6.1 LDA+DMFT

Although the Hubbard model is able to explain basic features of the phase diagram of correlated electrons it cannot explain the physics of real materials in any detail. Clearly, realistic theories must take into account the explicit electronic and lattice structure of the systems.

Until recently the electronic properties of solids were investigated by two essentially separate communities, one using model Hamiltonians in conjunction with many-body techniques, the other employing density functional theory (DFT) [62, 63]. DFT and its local density approximation (LDA) have the advantage of being *ab initio* approaches which do not require empirical

<sup>8</sup>Here we assume for simplicity that the metal remains a Fermi liquid, and the insulator stays paramagnetic, down to the lowest temperatures. In fact, a Cooper pair instability will eventually occur in the metal, and the insulator will become long-range ordered, too. In this case the slope  $dU/dT$  can change sign several times depending on the value of the entropy of the two phases across the phase transition.

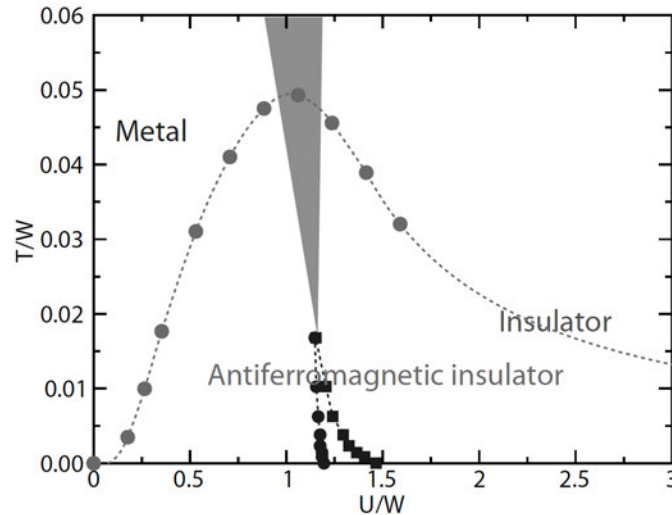


**Fig. 10:** On bipartite lattices and for half filling ( $n = 1$ ) the paramagnetic phase is unstable against antiferromagnetism. The metal-insulator transition is then completely hidden by the antiferromagnetic insulating phase; from Ref. [61].

parameters as input. Indeed, they are highly successful techniques for the calculation of the electronic structure of real materials [64]. However, in practice DFT/LDA is seriously restricted in its ability to describe strongly correlated materials where the on-site Coulomb interaction is comparable with the band width. Here, the model Hamiltonian approach is more general and powerful since there exist systematic theoretical techniques to investigate the many-electron problem with increasing accuracy. Nevertheless, the uncertainty in the choice of the model parameters and the technical complexity of the correlation problem itself prevent the model Hamiltonian approach from being a flexible or reliable enough tool for studying real materials. The two approaches are therefore complementary. In view of the individual power of DFT/LDA and the model Hamiltonian approach, respectively, it had always been clear that a combination of these techniques would be highly desirable for *ab initio* investigations of real materials, including, e.g., *f*-electron systems and Mott insulators. One of the first successful attempts in this direction was the LDA+U method [65, 66], which combines LDA with a basically static, i.e., Hartree-Fock-like, mean-field approximation for a multi-band Anderson lattice model (with interacting and non-interacting orbitals). This method proved to be a very useful tool in the study of long-range ordered, insulating states of transition metals and rare-earth compounds. However, the paramagnetic metallic phase of correlated electron systems such as high-temperature superconductors and heavy-fermion systems clearly requires a treatment that goes beyond a static mean-field approximation and includes dynamical effects, e.g., the frequency dependence of the self-energy.

Here the recently developed LDA+DMFT method — a new computational scheme which merges electronic band structure calculations and the dynamical mean-field theory [67–76, 30] — has proved to be a breakthrough. Starting from conventional band structure calculations in the local density approximation (LDA) the correlations are taken into account by the Hubbard interaction

and a Hund's rule coupling term. The resulting DMFT equations are solved numerically with a quantum Monte-Carlo (QMC) algorithm. By construction, LDA+DMFT includes the correct quasiparticle physics and the corresponding energetics. It also reproduces the LDA results in the limit of weak Coulomb interaction  $U$ . More importantly, LDA+DMFT correctly describes the correlation induced dynamics near a Mott-Hubbard MIT and beyond. Thus, LDA+DMFT and related approaches [77, 78] are able to account for the physics at all values of the Coulomb interaction and doping level.

In the LDA+DMFT approach the LDA band structure is expressed by a one-particle Hamiltonian  $\hat{H}_{\text{LDA}}^0$ , and is then supplemented by the local Coulomb repulsion  $U$  and Hund's rule exchange  $J$  (here we follow the presentation of Held *et al.* [72]). This leads to a material specific generalization of the one-band model Hamiltonian

$$\hat{H} = \hat{H}_{\text{LDA}}^0 + U \sum_m \sum_i \hat{n}_{im\uparrow} \hat{n}_{im\downarrow} + \sum_{i,m \neq m', \sigma, \sigma'} (V - \delta_{\sigma\sigma'} J) \hat{n}_{im\sigma} \hat{n}_{im'\sigma'}. \quad (30)$$

Here  $m$  and  $m'$  enumerate the three interacting  $t_{2g}$  orbitals of the transition metal ion or the  $4f$  orbitals in the case of rare earth elements. The interaction parameters are related by  $V = U - 2J$  which holds exactly for degenerate orbitals and is a good approximation for the  $t_{2g}$ . The actual values for  $U$  and  $V$  can be obtained from an averaged Coulomb parameter  $\bar{U}$  and Hund's exchange  $J$ , which can be calculated by constrained LDA.

In the one-particle part of the Hamiltonian

$$\hat{H}_{\text{LDA}}^0 = \hat{H}_{\text{LDA}} - \sum_i \sum_{m\sigma} \Delta\epsilon_d \hat{n}_{im\sigma}. \quad (31)$$

the energy term containing  $\Delta\epsilon_d$  is a shift of the one-particle potential of the interacting orbitals. It cancels the Coulomb contribution to the LDA results ("double-counting correction") and can also be calculated by constrained LDA [72].

Within the LDA+DMFT scheme the self-consistency condition connecting the self-energy  $\Sigma$  and the Green function  $G$  at frequency  $\omega$  reads:

$$G_{qm,q'm'}(\omega) = \frac{1}{V_B} \int d^3k \left( [\omega \mathbf{1} + \mu \mathbf{1} - H_{\text{LDA}}^0(\mathbf{k}) - \Sigma(\omega)]^{-1} \right)_{qm,q'm'}. \quad (32)$$

Here,  $\mathbf{1}$  is the unit matrix,  $\mu$  the chemical potential,  $H_{\text{LDA}}^0(\mathbf{k})$  is the orbital matrix of the LDA Hamiltonian derived, for example, in a linearized muffin-tin orbital (LMTO) basis,  $\Sigma(\omega)$  denotes the self-energy matrix which is nonzero only between the interacting orbitals, and  $[\dots]^{-1}$  implies the inversion of the matrix with elements  $n$  ( $=qm$ ),  $n'$  ( $=q'm'$ ), where  $q$  and  $m$  are the indices of the atom in the primitive cell and of the orbital, respectively. The integration extends over the Brillouin zone with volume  $V_B$  (we note that  $\hat{H}_{\text{LDA}}^0$  may include additional non-interacting orbitals).

For cubic transition metal oxides Eq. (32) can be simplified to

$$G(\omega) = G^0(\omega - \Sigma(\omega)) = \int d\epsilon \frac{N^0(\epsilon)}{\omega - \Sigma(\omega) - \epsilon} \quad (33)$$

if the degenerate  $t_{2g}$  orbitals crossing the Fermi level are well separated from the other orbitals. For non-cubic systems the degeneracy is lifted. In this case we employ Eq. (33) as an approximation, using different  $\Sigma_m(\omega)$ ,  $N_m^0(\epsilon)$  and  $G_m(\omega)$  for the three non-degenerate  $t_{2g}$  orbitals. The Hamiltonian (30) is solved within the DMFT using standard quantum Monte-Carlo (QMC) techniques [32] to solve the self-consistency equations. From the imaginary time QMC Green function one can calculate the physical (real frequency) spectral function with the maximum entropy method [79].

## 6.2 Single-particle spectrum of correlated electron materials

Transition metal oxides are an ideal laboratory for the study of electronic correlations in solids. Among these materials, cubic perovskites have the simplest crystal structure and thus may be viewed as a starting point for understanding the electronic properties of more complex systems. Typically, the  $3d$  states in those materials form comparatively narrow bands with width  $W \sim 2-3$  eV, which leads to strong Coulomb correlations between the electrons.

Photoemission spectra provide a direct experimental tool to study the electronic structure and spectral properties of electronically correlated materials. In particular, spectroscopic studies of strongly correlated  $3d^1$  transition metal oxides [80, 6, 5, 81–83] find a pronounced lower Hubbard band in the photoemission spectra which cannot be explained by conventional band structure theory. These are typical correlation effects which will now be illustrated by results obtained with the LDA+DMFT approach for the simple  $3d^1$  transition metal compounds  $\text{SrVO}_3$  and  $\text{CaVO}_3$ .

The main effect of the substitution of Sr ions in  $\text{SrVO}_3$  by the isovalent, but smaller, Ca ions is to decrease the V-O-V angle from  $\theta = 180^\circ$  in  $\text{SrVO}_3$  to  $\theta \approx 162^\circ$  in the orthorhombically distorted structure of  $\text{CaVO}_3$ . However, this rather strong bond bending results only in a 4% decrease of the one-particle bandwidth  $W$  and thus in a correspondingly small increase of the ratio  $U/W$  as one moves from  $\text{SrVO}_3$  to  $\text{CaVO}_3$ .

LDA+DMFT(QMC) spectra of  $\text{SrVO}_3$  and  $\text{CaVO}_3$  were calculated [5] by starting from the respective LDA DOS of the two materials; they are shown in Fig. 11. These spectra show genuine correlation effects, i.e., the formation of lower Hubbard bands at about 1.5 eV and upper Hubbard bands at about 2.5 eV, with well-pronounced quasiparticle peaks at the Fermi energy. Therefore both  $\text{SrVO}_3$  and  $\text{CaVO}_3$  are strongly correlated metals [5, 84]. The DOS of the two systems shown in Fig. 11 are quite similar. In fact,  $\text{SrVO}_3$  is slightly less correlated than  $\text{CaVO}_3$ , in accord with their different LDA bandwidths. The inset of Fig. 11 shows that the effect of temperature on the spectrum is small for  $T \lesssim 700$  K.

Since the three  $t_{2g}$  orbitals of this simple  $3d^1$  material are (almost) degenerate the spectral function has the same three-peak structure as that of the one-band Hubbard model shown in Fig. 8. The temperature induced decrease of the quasiparticle peak height is also clearly seen. As noted in Sec. 5 the actual form of the spectrum no longer resembles the input (LDA) DOS, i.e., it essentially depends only on the first three energy moments of the LDA DOS (electron density, average energy, band width).

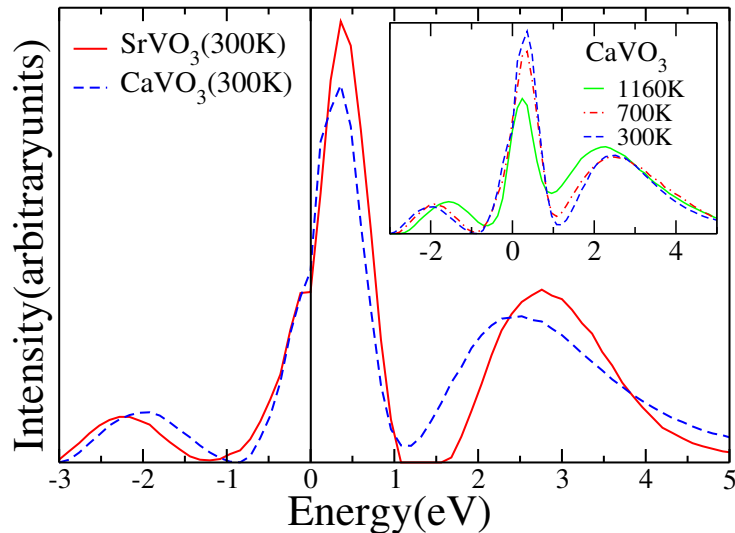


**Fig. 11:** LDA+DMFT(QMC) spectrum of  $\text{SrVO}_3$  (solid line) and  $\text{CaVO}_3$  (dashed line) calculated at  $T=300$  K; inset: effect of temperature in the case of  $\text{CaVO}_3$ ; after Ref. [5].

In the left panel of Fig. 12 the LDA+DMFT(QMC) spectra at 300K are compared with experimental high-resolution bulk PES; for details see ref. [85]. The quasiparticle peaks in theory and experiment are seen to be in very good agreement. In particular, their height and width are almost identical for both  $\text{SrVO}_3$  and  $\text{CaVO}_3$ . The difference in the positions of the lower Hubbard bands may be partly due to (i) the subtraction of the (estimated) oxygen contribution which might also remove some  $3d$  spectral weight below  $-2$  eV, and (ii) uncertainties in the *ab initio* calculation of the local Coulomb interaction strength. In the right panel of Fig. 12 comparison is made with XAS data [86]. Again, the overall agreement of the weights and positions of the quasiparticle and upper  $t_{2g}$  Hubbard band is good, including the tendencies when going from  $\text{SrVO}_3$  to  $\text{CaVO}_3$  ( $\text{Ca}_{0.9}\text{Sr}_{0.1}\text{VO}_3$  in the experiment). For  $\text{CaVO}_3$  the weight of the quasiparticle peak is somewhat lower than in the experiment. In contrast to one-band Hubbard model calculations, the material specific results reproduce the strong asymmetry around the Fermi energy with respect to weights and bandwidths. The slight differences in the quasiparticle peaks (see Fig. 11) lead to different effective masses, namely  $m^*/m = 2.1$  for  $\text{SrVO}_3$  and  $m^*/m = 2.4$  for  $\text{CaVO}_3$ . These theoretical values agree with  $m^*/m = 2 - 3$  for  $\text{SrVO}_3$  and  $\text{CaVO}_3$  as obtained from de Haas-van Alphen experiments and thermodynamics [87].

The experimentally determined spectra of  $\text{SrVO}_3$  and  $\text{CaVO}_3$  and the good agreement with parameter-free LDA+DMFT calculations confirm the existence of a pronounced three-peak structure in a correlated bulk material. Although the DMFT had predicted such a behavior for the Hubbard model (see Sec. 5.1.) it was not clear whether the DMFT result would really be able to describe real materials in three dimensions. Now it has been confirmed that the three-peak structure not only occurs in single-impurity Anderson models but also in three-dimensional correlated bulk matter.

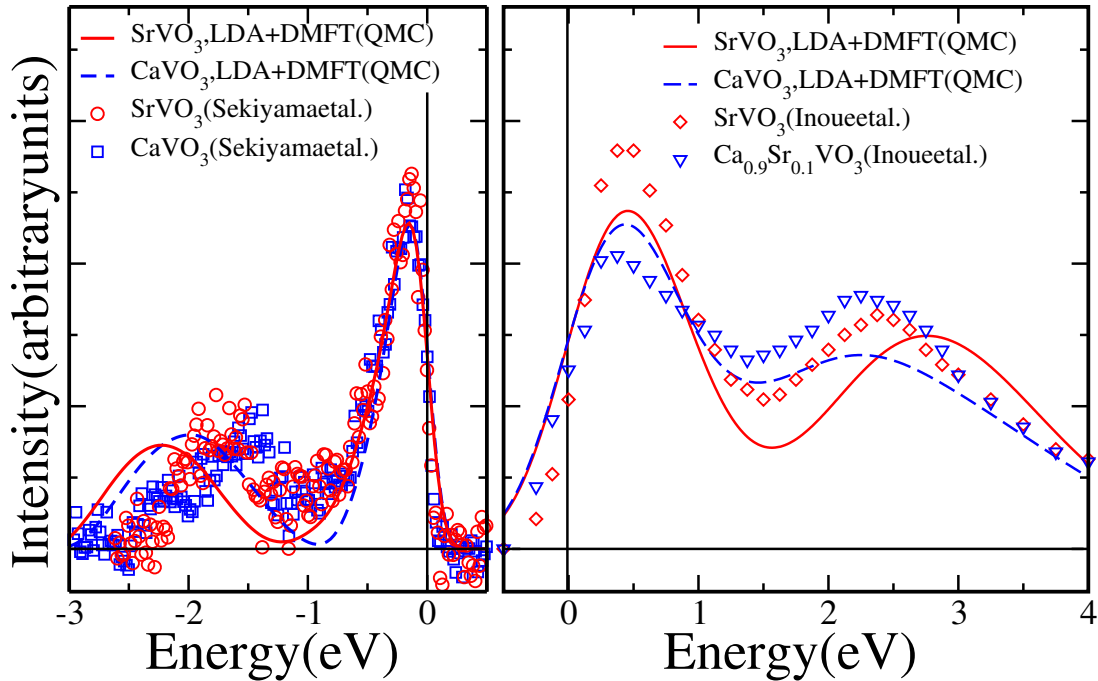


**Fig. 12:** Comparison of the calculated, parameter-free LDA+DMFT(QMC) spectra of SrVO<sub>3</sub> (solid line) and CaVO<sub>3</sub> (dashed line) with experiment. Left: Bulk-sensitive high-resolution PES (SrVO<sub>3</sub>: circles; CaVO<sub>3</sub>: rectangles). Right: XAS for SrVO<sub>3</sub> (diamonds) and Ca<sub>0.9</sub>Sr<sub>0.1</sub>VO<sub>3</sub> (triangles) [86]. Horizontal line: experimental subtraction of the background intensity; after Ref. [85].

## 7 Summary and outlook

Due to the intensive international research over the last two decades the DMFT has quickly developed into a powerful method for the investigation of electronic systems with strong correlations. It provides a comprehensive, non-perturbative and thermodynamically consistent approximation scheme for the investigation of finite-dimensional systems (in particular for dimension  $d = 3$ ), and is particularly useful for the study of problems where perturbative approaches are inapplicable. For this reason the DMFT has now become the standard mean-field theory for fermionic correlation problems, including cold atoms in optical lattices [88–92]. The study of models in non-equilibrium within a suitable generalization of the DMFT has become yet another fascinating new research area [93–101].

Until a few years ago research into correlated electron systems concentrated on homogeneous bulk systems. DMFT investigations of systems with internal or external inhomogeneities such as thin films and multi-layered nanostructures are still very new [102–107]. They are particularly important in view of the novel types of functionalities of such systems, which may have important applications in electronic devices. Here the DMFT and its generalizations will certainly be very useful.

In particular, the development of the *ab initio* band-structure calculation technique referred to as LDA+DMFT has proved to be a breakthrough in the investigation of electronically correlated

materials. It has already provided important insights into the spectral and magnetic properties of correlated electron materials, e.g., transition metals and their oxides. Clearly, this approach has a great potential for further developments. It is the goal of the DFG Research Unit on *Dynamical Mean-Field Approach with Predictive Power for Strongly Correlated Materials* which organizes this Autumn School “Hands-on LDA+DMFT” to develop the LDA+DMFT framework into a comprehensive *ab initio* approach which will be able to describe, and even predict, the properties of complex correlated materials.

## **Acknowledgment**

Support of the Deutsche Forschungsgemeinschaft through FOR1346 is gratefully acknowledged.

## References

- [1] J.H. de Boer and E.J.W. Verwey, Proc. Phys. Soc. **49**, No. **4S**, 59 (1937)
- [2] N.F. Mott and R. Peierls, Proc. Phys. Soc. A **49**, 72 (1937)
- [3] D.B. McWhan, A. Menth, J.P. Remeika, W.F. Brinkman, and T.M. Rice, Phys. Rev. B **B2**, 1920 (1973)
- [4] G.A. Sawatzky and J.W. Allen, Phys. Rev. Lett. **53**, 2339 (1984)
- [5] A. Sekiyama, H. Fujiwara, S. Imada, S. Suga, H. Eisaki, S.I. Uchida, K. Takegahara, H. Harima, Y. Saitoh, I.A. Nekrasov, G. Keller, D. E. Kondakov, A.V. Kozhevnikov, T. Pruschke, K. Held, D. Vollhardt, and V. I. Anisimov, Phys. Rev. Lett. **93**, 156402 (2004)
- [6] M. Imada, A. Fujimori, and Y. Tokura, Rev. Mod. Phys. **70**, 1039 (1998)
- [7] M.C. Gutzwiller, Phys. Rev. Lett. **10**, 159 (1963)
- [8] J. Hubbard, Proc. Roy. Soc. London **A276**, 238 (1963)
- [9] J. Kanamori, Prog. Theor. Phys. **30**, 275 (1963)
- [10] R.J. Baxter, *Exactly Solved Models in Statistical Mechanics* (Academic Press, London, 1982)
- [11] D. Vollhardt, in *Correlated Electron Systems*, edited by V.J. Emery (World Scientific, Singapore, 1993) p. 57; [http://www.physik.uni-augsburg.de/theo3/Research/research\\_jerusalem.vollha.en.shtml](http://www.physik.uni-augsburg.de/theo3/Research/research_jerusalem.vollha.en.shtml)
- [12] M. Eckstein, M. Kollar, K. Byczuk and D. Vollhardt, Phys. Rev. B **71**, 235119 (2005)
- [13] C. Itzykson and J.-M. Drouffe, *Statistical Field Theory* (Cambridge University Press, Cambridge, 1989)
- [14] R. Brout, Phys. Rev. **118**, 1009 (1960)
- [15] C.J. Thompson, Commun. Math. Phys. **36**, 255 (1974)
- [16] W. Metzner and D. Vollhardt, Phys. Rev. Lett. **62**, 324 (1989)
- [17] U. Wolff, Nucl. Phys. B **225**, 391 (1983)
- [18] E. Müller-Hartmann, Z. Phys. B **74**, 507 (1989)
- [19] W. Metzner, Z. Phys. B **77**, 253 (1989)
- [20] E. Müller-Hartmann, Z. Phys. B **76**, 211 (1989)
- [21] H. Schweitzer and G. Czycholl, Solid State Comm. **69**, 171 (1989)

- [22] U. Brandt and C. Mielsch, *Z. Phys.* **B 75**, 365 (1989)
- [23] P.G.J. van Dongen, F. Gebhard, and D. Vollhardt, *Z. Phys.* **76**, 199 (1989)
- [24] V. Janiš, *Z. Phys. B* **83**, 227 (1991)
- [25] V. Janiš and D. Vollhardt, *Int. J. Mod. Phys. B* **6**, 731 (1992)
- [26] A. Georges and G. Kotliar, *Phys. Rev. B* **45**, 6479 (1992)
- [27] M. Jarrell, *Phys. Rev. Lett.* **69**, 168 (1992)
- [28] Th. Pruschke, M. Jarrell, and J.K. Freericks, *Adv. Phys.* **44**, 187 (1995)
- [29] A. Georges, G. Kotliar, W. Krauth, and M.J. Rozenberg, *Rev. Mod. Phys.* **68**, 13 (1996)
- [30] G. Kotliar and D. Vollhardt, *Physics Today* **3**, 53 (2004)
- [31] D. Vollhardt, in *Lectures on the Physics of Strongly Correlated Systems XIV, AIP Conference Proceedings*, vol. 1297, ed. by A. Avella, F. Mancini (American Institute of Physics, Melville, 2010), p. 339; arXiv:1004.5069v3
- [32] J.E. Hirsch and R.M. Fye, *Phys. Rev. Lett.* **56**, 2521 (1986)
- [33] X.Y. Zhang, M.J. Rozenberg, and G. Kotliar, *Phys. Rev. Lett.* **70**, 1666 (1993)
- [34] J.K. Freericks and V. Zlatić, *Rev. Mod. Phys.* **75**, 1333 (2003)
- [35] M.J. Rozenberg, X.Y. Zhang, and G. Kotliar, *Phys. Rev. Lett.* **69**, 1236 (1992)
- [36] A. Georges and W. Krauth, *Phys. Rev. Lett.* **69**, 1240 (1992)
- [37] Th. Maier, M. Jarrell, Th. Pruschke, and M.H. Hettler, *Rev. Mod. Phys.* **77**, 1027 (2005)
- [38] E. Gull, A. J. Millis, A. I. Lichtenstein, A. N. Rubtsov, M. Troyer, P. Werner, *Rev. Mod. Phys.* **83**, 349 (2011)
- [39] R. Bulla, *Phys. Rev. Lett.* **83**, 136 (1999)
- [40] R. Bulla, T.A. Costi, and Th. Pruschke, *Rev. Mod. Phys.* **80**, 395 (2008)
- [41] M. Caffarel and W. Krauth, *Phys. Rev. Lett.* **72**, 1545 (1994)
- [42] Q. Si, M.J. Rozenberg, G. Kotliar, and A.E. Ruckenstein, *Phys. Rev. Lett.* **72**, 2761 (1994)
- [43] M.J. Rozenberg, G. Moeller, and G. Kotliar, *Mod. Phys. Lett. B* **8**, 535 (1994)
- [44] N.F. Mott, *Rev. Mod. Phys.* **40**, 677 (1968)
- [45] N.F. Mott, *Metal–Insulator Transitions* (Taylor and Francis, London, 1990), 2 edition

- 
- [46] F. Gebhard, *The Mott Metal-Insulator Transition*, Springer, Berlin, 1997
- [47] D.B. McWhan and J.P. Remeika, Phys. Rev. B **B2**, 3734 (1970)
- [48] T.M. Rice and D.B. McWhan, IBM J. Res. Develop. **251** (May 1970)
- [49] J. Hubbard, Proc. Roy. Soc. London **A281**, 401 (1964)
- [50] W.F. Brinkman and T.M. Rice, Phys. Rev. B **2**, 4302 (1970)
- [51] M.C. Gutzwiller, Phys. Rev. **137**, A1726 (1965)
- [52] W. Metzner and D. Vollhardt, Phys. Rev. B **37**, 7382 (1988)
- [53] D. Vollhardt, Rev. Mod. Phys. **56**, 99 (1984)
- [54] N. Blümer, *Metal-Insulator Transition and Optical Conductivity in High Dimensions* (Shaker Verlag, Aachen, 2003)
- [55] R. Bulla, T.A. Costi, and D. Vollhardt, Phys. Rev. B **64**, 045103 (2001)
- [56] D. Vollhardt, K. Held, G. Keller, R. Bulla, Th. Pruschke, I.A. Nekrasov, and V.I. Anisimov, J. Phys. Soc. Jpn. **74**, 136 (2005)
- [57] M.J. Rozenberg, R. Chitra, and G. Kotliar, Phys. Rev. Lett. **83**, 3498 (1999)
- [58] J. Joo and V. Oudovenko, Phys. Rev. B **64**, 193102 (2001)
- [59] D. Vollhardt and P. Wölfle, *The Superfluid Phases of Helium 3* (Taylor and Francis, London, 1990)
- [60] H. Park, K. Haule, and G. Kotliar, Phys. Rev. Lett. **101**, 186403 (2008)
- [61] Th. Pruschke, Prog. Theor. Phys. Suppl. **160**, 274 (2005)
- [62] P. Hohenberg and W. Kohn, Phys. Rev. **136B**, 864 (1964).
- [63] W. Kohn and L.J. Sham, Phys. Rev. **140**, A1133 (1965)
- [64] R.O. Jones and O. Gunnarsson, Rev. Mod. Phys. **61**, 689 (1989)
- [65] V.I. Anisimov, J. Zaanen, and O.K. Andersen, Phys. Rev. B **44**, 943 (1991)
- [66] V.I. Anisimov, F. Aryasetiawan, and A.I. Lichtenstein, J. Phys. Cond. Matter **9**, 767 (1997)
- [67] V.I. Anisimov, A.I. Poteryaev, M.A. Korotin, A.O. Anokhin, and G. Kotliar, J. Phys.: Cond. Matt. **9**, 7359 (1997)
- [68] A.I. Lichtenstein and M.I. Katsnelson, Phys. Rev. B **57**, 6884 (1998)

- [69] I.A. Nekrasov, K. Held, N. Blümer, A.I. Poteryaev, V.I. Anisimov, and D. Vollhardt, *Eur. Phys. J. B* **18**, 55 (2000)
- [70] K. Held, I.A. Nekrasov, N. Blümer, V.I. Anisimov, and D. Vollhardt, *Int. J. Mod. Phys. B* **15**, 2611 (2001)
- [71] A.I. Lichtenstein, M.I. Katsnelson, and G. Kotliar, in *Electron Correlations and Materials Properties*, edited by A. Gonis, N. Kioussis, and M. Ciftan (Kluwer Academic/Plenum, New York, 2002), p. 428
- [72] K. Held, I.A. Nekrasov, G. Keller, V. Eyert, N. Blümer, A.K. McMahan, R.T. Scalettar, T. Pruschke, V.I. Anisimov, and D. Vollhardt, *Psi-k Newsletter* **56**, 65 (2003); reprinted in *Phys. Status Solidi B* **243**, 2599 (2006)
- [73] G. Kotliar, S.Y. Savrasov, K. Haule, V.S. Oudovenko, O. Parcollet, C. A. Marianetti, *Rev. Mod. Phys.* **78**, 865 (2006)
- [74] K. Held, *Adv. Phys.* **56**, 829 (2007)
- [75] M.I. Katsnelson, V.Yu. Irkhin, L. Chioncel, A.I. Lichtenstein, and R.A. de Groot, *Rev. Mod. Phys.* **80**, 315 (2008)
- [76] J. Kuneš, I. Leonov, M. Kollar, K. Byczuk, V.I. Anisimov, and D. Vollhardt, *Eur. Phys. J. Special Topics* **180**, 5 (2010)
- [77] S. Biermann, F. Aryasetiawan, and A. Georges, *Phys. Rev. Lett.* **90**, 086402 (2003)
- [78] J. Minár, L. Chioncel, A. Perlov, H. Ebert, M.I. Katsnelson, and A.I. Lichtenstein, *Phys. Rev. B* **72**, 45125 (2005)
- [79] M. Jarrell and J.E. Gubernatis, *Phys. Rep.* **269**, 133 (1996)
- [80] A. Fujimori, I. Hase, H. Namatame, Y. Fujishima, Y. Tokura, H. Eisaki, S. Uchida, K. Takegahara, and F.M.F. de Groot, *Phys. Rev. Lett.* **69**, 1796 (1992)
- [81] S.-K. Mo, H.-D. Kim, J.W. Allen, G.H. Gweon, J.D. Denlinger, J.-H. Park, A. Sekiyama, A. Yamasaki, S. Suga, P. Metcalf, and K. Held, *Phys. Rev. Lett.* **93**, 076404 (2004)
- [82] D. Schrupp, M. Sing, M. Tsunekawa, H. Fujiwara, S. Kasai, A. Sekiyama, S. Suga, T. Muro, V.A.M. Brabers, and R. Claessen, *Europhys. Lett.* **70**, 789 (2005)
- [83] T. C. Koethe, Z. Hu, M.W. Haverkort, C. Schüßler-Langeheine, F. Venturini, N.B. Brookes, O. Tjernberg, W. Reichelt, H.H. Hsieh, H.-J. Lin, C.T. Chen, and L.H. Tjeng, *Phys. Rev. Lett.* **97**, 116402 (2006)
- [84] E. Pavarini, S. Biermann, A. Poteryaev, A.I. Lichtenstein, A. Georges, and O.K. Andersen, *Phys. Rev. Lett.* **92**, 176403 (2004)

- 
- [85] I.A. Nekrasov, G. Keller, D.E. Kondakov, A.V. Kozhevnikov, Th. Pruschke, K. Held, D. Vollhardt, and V.I. Anisimov, *Phys. Rev. B* **72**, 155106 (2005)
- [86] I.H. Inoue, I. Hase, Y. Aiura, A. Fujimori, K. Morikawa, T. Mizokawa, Y. Haruyama, T. Maruyama, and Y. Nishihara, *Physica C* **235-240**, 1007 (1994)
- [87] I.H. Inoue, C. Bergemann, I. Hase, and S.R. Julian, *Phys. Rev. Lett.* **88**, 236403 (2002)
- [88] A. Rapp, G. Zarand, C. Honerkamp, W. Hofstetter, *Phys. Rev. Lett.* **98**, 160405 (2007)
- [89] M. Snoek, I. Titvinidze, C. Toke, K. Byczuk, and W. Hofstetter, *New J. Phys.* **10**, 093008 (2008)
- [90] R. Jördens, N. Strohmaier, K. Günter, H. Moritz, and T. Esslinger, *Nature* **455**, 204 (2008)
- [91] U. Schneider, L. Hackermüller, S. Will, Th. Best, I. Bloch, T.A. Costi, R.W. Helmes, D. Rasch, A. Rosch, *Science* **322**, 1520 (2008)
- [92] I. Bloch, J. Dalibard, and W. Zwerger, *Rev. Mod. Phys.* **80**, 885 (2008)
- [93] V. Turkowski and J.K. Freericks, *Phys. Rev. B* **71**, 085104 (2005)
- [94] J.K. Freericks, V.M. Turkowski, and V. Zlatić, *Phys. Rev. Lett.* **97** 266408 (2006)
- [95] J.K. Freericks, *Phys. Rev. B* **77**, 075109 (2008)
- [96] N. Tsuji, T. Oka, and H. Aoki, *Phys. Rev. B* **78**, 235124 (2008)
- [97] M. Eckstein, and M. Kollar, *Phys. Rev. Lett.* **100**, 120404 (2008)
- [98] M. Eckstein, and M. Kollar, *Phys. Rev. B* **78**, 205119 (2008)
- [99] J.K. Freericks, H.R. Krishnamurthy, and Th. Pruschke, *Phys. Rev. Lett.* **102**, 136401 (2009)
- [100] M. Eckstein, M. Kollar, and P. Werner, *Phys. Rev. Lett.* **103**, 056403 (2009)
- [101] M. Eckstein and P. Werner, *Phys. Rev. B* **82**, 115115 (2010)
- [102] M. Potthoff and W. Nolting, *Phys. Rev. B* **59**, 2549 (1999)
- [103] J.K. Freericks, *Transport in multilayered nanostructures — The dynamical mean-field approach* (Imperial College Press, London, 2006)
- [104] M. Takizawa, H. Wadati, K. Tanaka, M. Hashimoto, T. Yoshida, A. Fujimori, A. Chikamtsu, H. Kumigashira, M. Oshima, K. Shibuya, T. Mihara, T. Ohnishi, M. Lippmaa, M. Kawasaki, H. Koinuma, S. Okamoto, and A.J. Millis, *Phys. Rev. Lett.* **97**, 057601 (2006)

- [105] L. Chen and J.K. Freericks, Phys. Rev. B **75**, 1251141 (2007)
- [106] K. Byczuk, in *Condensed Matter Physics in the Prime of the 21st Century: Phenomena, Materials, Ideas, Methods*, ed. J. Jedrzejewski (World Scientific, Singapore, 2008), p. 1
- [107] R.W. Helmes, T.A. Costi, and A. Rosch, Phys. Rev. Lett. **100**, 056403 (2008)